

Classification: Physical sciences, chemistry

## Dynamic force spectroscopy of synthetic oligorotaxane foldamers

Damien Sluysmans<sup>a</sup>, Floriane Devaux<sup>a</sup>, Carson Bruns<sup>b</sup>, J. Fraser Stoddart<sup>b</sup>, Anne-Sophie Duwez<sup>\*a</sup>

<sup>a</sup>UR Molecular Systems, University of Liège, 4000 Liège, Belgium.

<sup>b</sup>Department of Chemistry, Northwestern University, Evanston, Illinois 60208-3113, USA.

\*Correspondence to:

Quartier Agora, Allée du 6 août 15 (B6a),

4000 Liège (Belgium)

[asduwez@ulg.ac.be](mailto:asduwez@ulg.ac.be)

+32 (0) 4 366 3482

Keywords: molecular machines, foldamers, single-molecule force spectroscopy, equilibrium dynamics

1 ***ABSTRACT (250 words – no references or fully cited)***

2 Wholly synthetic molecules involving both mechanical bonds and a folded secondary  
3 structure are one of the most promising architectures for the design of functional molecular  
4 machines with unprecedented properties. Here, we report dynamic single-molecule force  
5 spectroscopy experiments that explore the energetic details of donor-acceptor oligorotaxane  
6 foldamers, a class of molecular switches. The mechanical breaking of the donor-acceptor  
7 interactions responsible for the folded structure shows a high constant rupture force over a  
8 broad range of loading rates, covering three orders of magnitude. In comparison with dynamic  
9 force spectroscopy performed during the past 20 years on various (bio)molecules, the near-  
10 equilibrium regime of oligorotaxanes persists at much higher loading rates, at which  
11 biomolecules have reached their kinetic regime, illustrating the very fast dynamics and  
12 remarkable rebinding capabilities of the intramolecular donor-acceptor interactions. We  
13 focused on one single interaction at a time and probed the stochastic rupture and rebinding  
14 paths. Using the Crooks fluctuation theorem, we measured the mechanical work produced  
15 during the breaking and rebinding to determine a free-energy difference,  $\Delta G$ , of  $6 \text{ kcal}\cdot\text{mol}^{-1}$   
16 between the two local conformations around a single bond.

17

18 ***SIGNIFICANCE STATEMENT (120 words)***

19 Donor-acceptor oligorotaxane foldamers are a class of molecular switches elegantly  
20 incorporating mechanical bonds in a folded molecular architecture. Such examples of  
21 foldamers are very rare, leaving the question wide open regarding what might emerge from a  
22 synergistic combination of mechanically interlocked molecules and foldamers. Here, using  
23 AFM-based dynamic single-molecule force spectroscopy, we mechanically drive  
24 oligorotaxanes out-of-equilibrium at a wide range of loading rates and observe their  
25 exceptional refolding capabilities and the very fast dynamics of the process. The near-

26 equilibrium pulling-relaxing cycles were exploited to determine the energy required to break  
27 one single donor-acceptor interaction from the distribution of work trajectories using  
28 fluctuation theorems. Our findings highlight the importance of molecular design on the  
29 performance of artificial molecular machines.  
30

31 **INTRODUCTION**

32 Biological molecular machines are known to operate out of their thermodynamic equilibrium  
33 in order to carry out specific tasks such as cargo transport performed by single myosins (1), or  
34 cell movements driven by flagella rotary motions (2). The work performed by these natural  
35 molecular motors is related to their dynamics in solution, and to the force exerted by the  
36 molecule to drive the relevant process in one direction. The invention of synthetic routes to  
37 wholly artificial molecular machines with highly precise and controlled architectures have led  
38 to the production of amazing molecules able to perform mechanical tasks (3–7). Their  
39 integration into materials, such as metal-organic frameworks (8) or polymer gels (9, 10), has  
40 been described recently. The resulting materials can experience a macroscopic change when  
41 each single machine is pulled out of its equilibrium state, as a result of an external stimulus,  
42 such as light irradiation or a change in solvent.

43 Collecting information about the behavior of such molecules when driven out of their  
44 equilibrium is crucial for the design of more efficient molecular devices. Atomic force  
45 microscopy (AFM)-based single-molecule force spectroscopy (SMFS) has emerged as a very  
46 elegant technique to probe inter- and intramolecular forces as well as mechanical processes  
47 (11–16). By trapping individual molecules between a mechanical probe and a substrate, it is  
48 possible to apply an external force to drive them out of the equilibrium and perform very  
49 precise and controlled operations in one direction. For 20 years, AFM-based SMFS was used  
50 to unravel the behavior of natural biomolecules under mechanical load and has led to a  
51 description of their stability, dynamics, and eventually their working processes (17–19).

52 Beyond standard force spectroscopy experiments, dynamic force spectroscopy, which is  
53 concerned with the influence of the loading rate on the force required to break the probed  
54 interaction, has been the subject of many theoretical and experimental studies (16, 20–24). It  
55 allows us to estimate kinetic off-rates and distances to transition states describing the involved

56 individual bonds from out-of-equilibrium single-molecule experiments. The evolution of the  
57 rupture force against the loading rate is described by several models, namely Bell-Evans (22),  
58 Friddle-Noy-De Yoreo (23), and Dudko-Hummer-Szabo (24).

59 By performing successive controlled pulling-relaxing cycles on individual molecules, it is  
60 also possible to reveal their singular behaviors under various mechanical loads and to measure  
61 the work performance needed to regain their initial conformation (19). One can evaluate if  
62 molecules are effective at absorbing energy from thermal fluctuations in the environment. The  
63 stochastic behavior of small molecules in an environment governed by random thermal  
64 fluctuations forces us to use theories of nonequilibrium statistic mechanics, known as  
65 fluctuation theorems (25–29), to uncover that part of the work which is reversible and thus  
66 deduce energetics information about the probed interactions. For example, the Crooks  
67 fluctuation theorem (29) was used to correlate the work measured during the mechanical  
68 unfolding and refolding of a RNA hairpin to the free-energy difference ( $\Delta G$ ) between both  
69 conformations (30), or to extract the free-energy differences between both conformations of  
70 an hydrogen-bonded [2]rotaxane (31).

71 Here, we have investigated the dynamics and the stochastic behavior of single donor-acceptor  
72 oligorotaxane foldamers, prototypes of artificial molecular switches, and extracted energetics  
73 information. The molecules are made of oligomeric backbone components incorporating 1,5-  
74 dioxynaphthalene (DNP) units encircled by tetracationic cyclobis(paraquat-*p*-phenylene)  
75 rings (CBPQT<sup>4+</sup>, Blue Boxes) (32–34). These oligorotaxanes are known to adopt a robust  
76 serpentine-like folded conformation (as depicted in Fig. 1A and B), stabilized by  
77 intramolecular noncovalent bonding interactions such as strong donor-acceptor  $\pi$ -interactions  
78 and hydrogen bonds linking the electron-donor DNP recognition sites and the electron-poor  
79 4,4'-bipyridinium dication (BIPY<sup>2+</sup>) of the Blue Boxes (32–35).

80

81 **RESULTS AND DISCUSSION**

82 **Dynamic force spectroscopy.** [4]- and [7]rotaxane foldamers (Fig. 1A and B) were grafted  
83 on gold-coated substrates following our previously published procedure (31) to obtain isolated  
84 single molecules, which were stretched mechanically using AFM-based single-molecule force  
85 spectroscopy (Fig. 1C). The force-extension curves obtained in dimethylformamide (DMF), a  
86 good solvent for the molecules, show a characteristic unfolding profile (Fig. 2) with regularly  
87 spaced force peaks, each separated by 2.4 nm on the basis of worm-like chain fits (see SI for  
88 details). The distance between the peaks nicely matches the theoretical distance expected for  
89 the sequential mechanical breaking of intramolecular donor-acceptor DNP-BIPY<sup>2+</sup>  
90 interactions on both sides of the ring. Rupture force values were also compiled in histograms  
91 (Fig. 2C and D) and show a most probable population at around 100 pN. The last peak  
92 displays a higher force, characteristic of an S–S interaction with gold (36). We performed  
93 standard SMFS experiments at 11 different loading rates (from  $6 \times 10^2$  to  $4 \times 10^5$  pN·s<sup>-1</sup>) to  
94 cover three orders of magnitude. At each loading rate, characteristic unfolding profiles were  
95 recovered and rupture force distributions were constructed (Fig. S1). The dynamic force  
96 spectrum of the [4]rotaxane, relating the evolution of the most probable rupture force ( $F$ ) with  
97 the associated loading rate ( $r$ ), is shown in Fig. 3. We observe a quasi-linearity of the rupture  
98 force with respect to the loading rate, suggesting a rate independent rupture force and thus  
99 providing evidence for the near-equilibrium regime of the experiment. Friddle and coworkers  
100 (23) have shown that a bond can be pulled in a near-equilibrium regime, at low loading rates,  
101 as the pulling rate approaches its natural dissociation rate. In this case, the bond is not affected  
102 by the external load and the average force required to break the interaction is constant ( $F_{eq}$ ).  
103 On the contrary, a bond pulled at a rate higher than its dissociation rate resists this mechanical  
104 stimulus, leading to a rupture force increase. This behavior corresponds to the out-of-  
105 equilibrium regime. The Friddle-Noy-De Yoreo model has been employed (23) successfully

106 to describe previous pulling experiments performed on numerous biomolecules and it has  
107 been shown that the rupture forces experienced at various loading rates can be described by a  
108 non-linear fit including both the near-equilibrium (loading rate independent) and the kinetic  
109 regimes where the force is proportional to the logarithm of the loading rate, as described by  
110 Evans (22). All the biomolecules studied by dynamic force spectroscopy and fitted by  
111 Friddle-Noy-De Yoreo model (Fig. 4) show a clear kinetic regime for loading rates varying  
112 from  $10^2$  to  $10^6$  pN·s<sup>-1</sup> (23). Here, for the stretching of the oligorotaxanes, we do not observe  
113 an increase of the rupture force within a similar range of loading rates (Fig. 4). The kinetic  
114 regime of the oligorotaxane is not reached yet at the highest loading rates. The equilibrium  
115 force determined  $F_{eq} = 108.1 \pm 1.2$  pN is high in comparison with the equilibrium force  
116 measured previously on natural biomolecules, supporting the high strength of the  
117 intramolecular donor-acceptor interactions. Compared to previous DFS studies performed on  
118 the same range of loading rates, we show here that the near-equilibrium regime of this  
119 synthetic molecule persists at much higher loading rates, demonstrating the very fast  
120 dynamics of the probed interaction. We attribute this extraordinary behavior to the proximity  
121 of the binding partners and the presence of mechanical bonds (37). They keep both  
122 intramolecular partners in close proximity and favorable orientation after the breaking of the  
123 interaction, making it easier to reform the bonds rapidly.

124

125 **Near-equilibrium stochastic behavior.** Even if the pulling experiments were performed near  
126 thermodynamic equilibrium, small molecules are always being submitted to random thermal  
127 fluctuations that constantly modify their unfolding and refolding paths (25). We performed  
128 single-molecule pulling-relaxing cycles at low loading rates (2500 and 5000 pN·s<sup>-1</sup>). The  
129 comparison between successive pulling and relaxing force curves evidenced the stochastic  
130 behavior of individual oligorotaxanes under mechanical load (Fig. 5 A-I). The work done to

131 unfold the molecule is not dissipated into the environment and is fully recovered in the  
132 refolding process, to remake the broken interactions. Fig. 5 A-B show the unfolding of several  
133 units. The relaxing curves point to the reformation of the previously broken interactions. By  
134 looking at one interaction at a time (Fig. 5 D-I), several patterns can be identified. In Fig. 5 D,  
135 the relaxing curve is identical to the stretching curve without any hysteresis, whereas  
136 hysteresis between pulling and relaxing curves can be observed in Fig. 5 E. Hysteresis  
137 indicates that the work done on the oligorotaxane during pulling is not fully recovered during  
138 relaxation and was dissipated. With smaller pulling rates, the system approaches quasi-static  
139 pulling, so that hysteresis disappears. Even if the dynamic force spectroscopy experiments  
140 (Fig. 3) performed on this system indicate that, for most pulling experiments, the near-  
141 equilibrium regime is attained on the average, we can distinguish singular stochastic behavior  
142 of individual molecules when stretched at low loading rates. Among these, we observe the  
143 simultaneous rupture of two interactions followed by the sequential reforming of each  
144 interaction separately (two peaks in the relaxing curve) (Fig. 5 F). Interestingly, fluctuations  
145 between folded and unfolded states appear in some pulling and relaxing curves (Fig. 5 G-I).  
146 These fluctuations are the signature of an experiment performed near the thermodynamic  
147 equilibrium of the probed interaction. It is thus consistent with the loading rate independent  
148 rupture force evidenced above. In Fig. 5 H, a peak in the relaxing curve, corresponding to the  
149 reformation of an interaction, appears with a ‘negative hysteresis’ compared to the breaking  
150 peak in the pulling curve. This observation can be explained by the consumption of thermal  
151 energy by the molecule to refold back to its previous state, hence exhibiting negative  
152 dissipated work. Such non-equilibrium trajectories with  $W_{\text{diss}} \leq 0$  can indeed exist (25).  
153 Strictly speaking, this observation is not a violation of the second law of thermodynamics  
154 when we consider the system as ‘the molecule *plus* the environment’. Nevertheless, this

155 situation is a clear example of a molecule taking advantage of the random thermal fluctuations  
156 ( $k_B T$ ) to induce a molecular movement and then recreate an intramolecular interaction.

157

158 **Determination of  $\Delta G$  between locally unfolded and folded states.** For a reversible process,  
159 the mechanical work equals the Gibbs free-energy change of the process, but the distribution  
160 of work trajectories (see Fig. 6) typically results in hysteresis because of the fluctuations.  
161 Recent developments in non-equilibrium statistical mechanics enable the recovery of the  
162 reversible work, and thus the zero-force free energy, from the distribution of work trajectories  
163 in pulling–relaxing cycles (30). In order to evaluate the energy required to break one DNP-  
164 BIPY<sup>2+</sup> interaction, the experiments were designed to probe only one interaction at a time. In  
165 order to measure the work performed during the breaking of a single interaction in the pulling  
166 step, we measured the area under the ‘force vs distance’ curve between the rupture distance  
167 and the distance where the molecule is back under tension,  $\Delta d$  (Fig. S2). This area was subject  
168 to correction by withdrawing the entropic contribution resulting from the stretching of the  
169 main chain (see details in SI). The same measurement was carried out for the relaxing step in  
170 order to determine the work performed by the molecule to reform the interaction. The  
171 distribution of  $\Delta d$  shows a main population centered at  $1.1 \pm 0.1$  nm (Fig. S3), an observation  
172 which confirms that a single interaction is being probed. The distributions of work of  
173 unfolding (during pulling) and folding (during relaxation) are shown in Fig. 6. They reveal a  
174 large overlapping region, confirming the near-equilibrium regime in this range of loading  
175 rates and a small amount of work being dissipated during the overall process. When the work  
176 done on a system ( $W$ ) is completely recovered in the reverse process ( $-W$ ), the Crooks  
177 fluctuation theorem states that  $W = \Delta G$  (29). Therefore, the conformational free-energy  
178 difference between locally unfolded and folded states was determined graphically where both  
179 forward and reverse works have the same value, at  $W = 10 \pm 2$   $k_B T$  (red line in Fig. 6).

180 Therefore, the energy required to break a single DNP-BIPY<sup>2+</sup> interaction,  $\Delta G$ , is equal  
181 to  $6 \pm 1$  kcal·mol<sup>-1</sup>. This value is in very good agreement with the theoretical  $\Delta G$  value  
182 calculated previously (38, 39).

183

## 184 **CONCLUSION**

185 For more than 20 years, single-molecule force spectroscopy has proved to be a powerful tool  
186 to manipulate single molecules and obtain exquisite information about their mechanical  
187 behavior. The technique has been widely used to determine equilibrium thermodynamic  
188 parameters by mechanically driving probed molecules out-of-equilibrium at various loading  
189 rates (16, 20–24). To date, there have been very few investigations reported on wholly  
190 synthetic small molecules (31, 40–44), mainly because of the difficulty of preparing  
191 appropriate molecules that can be interfaced with single-molecule force spectroscopy  
192 techniques, but also because the size of the molecules implies that the rupture events occur at  
193 very small distances, in the range of one nanometer. Here we have probed donor-acceptor  
194 oligorotaxane foldamers, synthetic prototypes of molecular switches, by AFM-based dynamic  
195 force spectroscopy. Our results demonstrate that the rupture force of the interactions  
196 responsible for the folding is not dependent on the loading rate over a huge range of values,  
197 from  $6 \times 10^2$  up to  $4 \times 10^5$  pN·s<sup>-1</sup>, a range at which a large variety of intramolecular systems  
198 display non-linear force spectra. This unique behavior reveals fast bond reforming, even for  
199 very high loading rates, and provides evidence for the wide range near-equilibrium regime of  
200 the probed interactions. We suggest that this behavior relies on the specific nature of the  
201 structure and superstructure of the oligorotaxanes. The proximity of the binding partners and  
202 the presence of mechanical bonds keep both intramolecular partners in close proximity and  
203 favorable orientations after the breaking of the interaction, making it easier to reform the  
204 bonds rapidly. Our results highlight the remarkable robustness of the intramolecular donor-

205 acceptor interactions. The near-equilibrium conditions allowed us to use the Crooks  
206 fluctuation theorem to recover the reversible work, and thus the free energy, from the  
207 distribution of work trajectories in pulling–relaxing cycles. We determined the free-energy  
208 difference,  $\Delta G$ , between locally folded and unfolded conformations, corresponding to the  
209 energy required to break one intramolecular DNP-BIPY<sup>2+</sup> interaction.

210 Our findings highlight the importance of the molecular design in the synthesis of efficient  
211 molecular machines, able to compete with or even surpass the performance of natural  
212 machines.

213

214 **MATERIALS AND METHODS**

215 The [4]- and [7]rotaxanes were synthesized according to protocols described previously (32).  
216 Briefly, one-pot syntheses use copper-catalyzed azide-alkyne cycloadditions to thioctic ester-  
217 functionalized stoppers at both ends of the DNP-derived polyether chains in the presence of  
218 CBPQT<sup>4+</sup> rings. Using conventional chromatographic techniques, oligorotaxanes with half the  
219 DNP units encircled by rings were isolated. The compounds were characterized by mass  
220 spectrometry and NMR spectroscopy (32).

221 The oligorotaxanes were grafted onto gold-coated silicon substrates using our previously  
222 established method (31) to obtain a sparse regime of the molecule of interest. The substrates  
223 were dipped for 1 h in a solution of the oligorotaxane ( $2 \times 10^{-8}$  mol) containing 90 mol% of  
224 dodecyl disulfide in Me<sub>2</sub>CO at room temperature. The role of the dodecyl disulfide is to  
225 ensure a dilute distribution of the oligorotaxanes on the surface as well as passivate the  
226 substrate. All the details are given in SI.

227 Single-molecule force spectroscopy experiments were carried out with a PicoPlus 5500  
228 microscope (Agilent Technologies), equipped with a closed-loop scanner. Gold-coated tips  
229 (OBL-10 Biolever, Bruker; nominal spring constant  $k = 0.009\text{--}0.1 \text{ N}\cdot\text{m}^{-1}$ ) were used for all  
230 the force experiments. The spring constant of each cantilever was calibrated by the thermal  
231 noise and Sader methods (45, 46). The molecules were picked up for force experiments by  
232 gently pressing the AFM tip against the substrate. Pulling–relaxing cycles were realized using  
233 a custom-made routine to guide the tip. Each force curve contains 20,000 data points. All the  
234 details are given in SI.

235

236 **ACKNOWLEDGEMENTS**

237 D. S. thanks the Fonds de la Recherche Scientifique-Fonds National pour la Recherche  
238 Scientifique (FRS-FNRS) for his FRIA fellowship. The research was supported by the project  
239 PDR T.0244.16 of the FRS-FNRS at University of Liège and by the King Abdulaziz City of  
240 Science and Technology (KACST) as part of their Joint Center of Excellence in Integrated  
241 Nano-Systems (JCIN) at Northwestern University.

242

243 **REFERENCES (all authors for submission)**

- 244 1. Kinbara K, Aida T (2005) Toward intelligent molecular machines: Directed motions of  
245 biological and artificial molecules and assemblies. *Chem Rev* 105(4):1377–1400.
- 246 2. Berg HC (2003) The rotary motor of bacterial flagella. *Annu Rev Biochem* 72(1):19–  
247 54.
- 248 3. Kay ER, Leigh DA, Zerbetto F (2007) Synthetic molecular motors and mechanical  
249 machines. *Angew Chem Int Ed* 46(1+2):72–191.
- 250 4. Kay ER, Leigh DA (2015) Rise of the molecular machines. *Angew Chem Int Ed*  
251 54(35):10080–10088.
- 252 5. Erbas-Cakmak S, Leigh DA, McTernan CT, Nussbaumer AL (2015) Artificial  
253 molecular machines. *Chem Rev* 115(18):10081–10206.
- 254 6. Mattia E, Otto S (2015) Supramolecular systems chemistry. *Nat Nanotechnol*  
255 10(2):111–119.
- 256 7. Bruns CJ, Stoddart JF (2016) Molecular switches and machines with mechanical  
257 bonds. *The Nature of the Mechanical Bond* (John Wiley & Sons, Inc., Hoboken, NJ,  
258 USA), pp 555–733.
- 259 8. Zhu K, O’Keefe CA, Vukotic VN, Schurko RW, Loeb SJ (2015) A molecular shuttle  
260 that operates inside a metal–organic framework. *Nat Chem* 7(6):514-519.

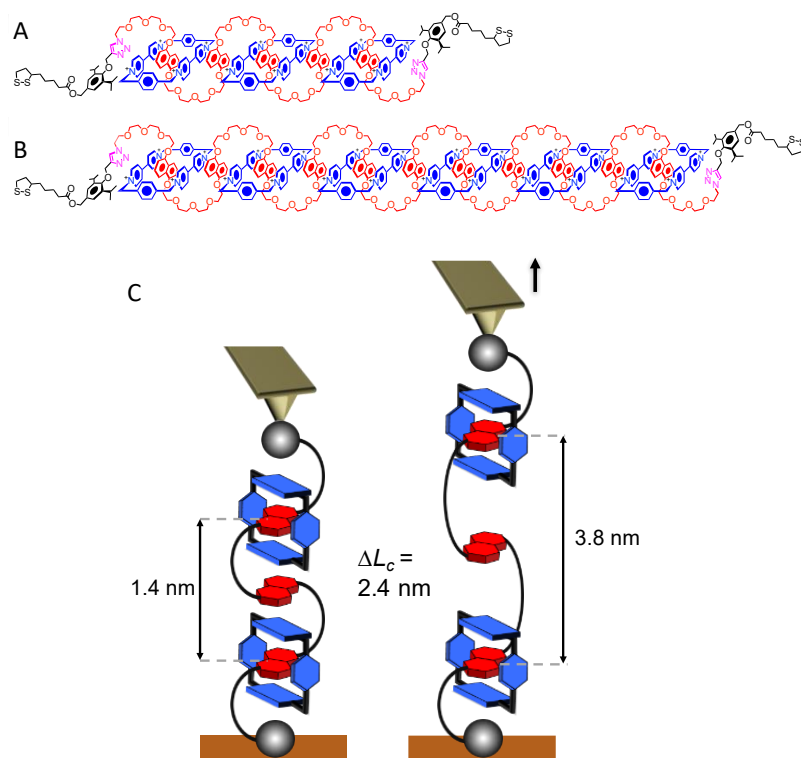
- 261 9. Li Q, Fuks G, Moulin E, Maaloum M, Rawiso M, Kulic I, Foy JT, Giuseppone N  
262 (2015) Macroscopic contraction of a gel induced by the integrated motion of light-  
263 driven molecular motors. *Nat Nanotechnol* 10(2):161–165.
- 264 10. Foy JT, Li Q, Goujon A, Colart-Itte J-R, Fuks G, Moulin E, Schiffmann O, Dattler D,  
265 Funeriu DP, Giuseppone N (2017) Dual-light control of nanomachines that integrate  
266 motor and modulator subunits. *Nat Nanotechnol* 12(6):540–545.
- 267 11. Fisher TE, Marszalek PE, Fernandez JM (2000) Stretching single molecules into novel  
268 conformations using the atomic force microscope. *Nat Struct Biol* 7(9):719–724.
- 269 12. Neuman KC, Nagy A (2008) Single-molecule force spectroscopy: Optical tweezers,  
270 magnetic tweezers and atomic force microscopy. *Nat Methods* 5(6):491–505.
- 271 13. Puchner EM, Gaub HE (2009) Force and function: probing proteins with AFM-based  
272 force spectroscopy. *Curr Opin Struct Biol* 19(5):605–614.
- 273 14. Duwez A-S, Willet N (2012) *Molecular Manipulation with Atomic Force Microscopy*.  
274 (CRC Press, Boca Raton).
- 275 15. Noy A (2008) *Handbook of Molecular Force Spectroscopy* ed Noy A (Springer US,  
276 Boston, MA).
- 277 16. Noy A (2011) Force spectroscopy 101: how to design, perform, and analyze an AFM-  
278 based single molecule force spectroscopy experiment. *Curr Opin Chem Biol*  
279 15(5):710–718.
- 280 17. Clausen-Schaumann H, Seitz M, Krautbauer R, Gaub HE (2000) Force spectroscopy  
281 with single bio-molecules. *Curr Opin Chem Biol* 4(5):524–530.
- 282 18. Borgia A, Williams PM, Clarke J (2008) Single-molecule studies of protein folding.  
283 *Annu Rev Biochem* 77(1):101–125.
- 284 19. Scholl ZN, Li Q, Marszalek PE (2014) Single molecule mechanical manipulation for  
285 studying biological properties of proteins, DNA, and sugars. *Wiley Interdiscip Rev*

- 286        *Nanomedicine Nanobiotechnology* 6(3):211–229.
- 287 20. Hughes ML, Dougan L (2016) The physics of pulling polyproteins: A review of single  
288 molecule force spectroscopy using the AFM to study protein unfolding. *Reports Prog*  
289 *Phys* 79(7):76601.
- 290 21. Friedsam C, Wehle AK, Kuehner F, Gaub HE (2003) Dynamic single-molecule force  
291 spectroscopy: Bond rupture analysis with variable spacer length. *J Phys Condens*  
292 *Matter* 15(18):S1709–S1723.
- 293 22. Evans E, Ritchie K (1997) Dynamic strength of molecular adhesion bonds. *Biophys J*  
294 72(4):1541–1555.
- 295 23. Friddle RW, Noy A, De Yoreo JJ (2012) Interpreting the widespread nonlinear force  
296 spectra of intermolecular bonds. *Proc Natl Acad Sci* 109(34):13573–13578.
- 297 24. Dudko OK, Hummer G, Szabo A (2008) Theory, analysis, and interpretation of single-  
298 molecule force spectroscopy experiments. *Proc Natl Acad Sci* 105(41):15755–15760.
- 299 25. Sevick E M, Prabhakar R, Williams S R, Searles D J (2008) Fluctuation theorems.  
300 *Annu Rev Phys Chem* 59:603–633.
- 301 26. Astumian RD (2006) The unreasonable effectiveness of equilibrium theory for  
302 interpreting nonequilibrium experiments. *Am J Phys* 74(8):683–688.
- 303 27. Jarzynski C (1997) Nonequilibrium equality for free energy differences. *Phys Rev Lett*  
304 78(14):2690–2693.
- 305 28. Jarzynski C (1997) Equilibrium free-energy differences from nonequilibrium  
306 measurements: A master-equation approach. *Phys Rev E* 56(5):5018–5035.
- 307 29. Crooks GE (1999) Entropy production fluctuation theorem and the nonequilibrium  
308 work relation for free energy differences. *Phys Rev E* 60(3):2721–2726.
- 309 30. Collin D, Ritort F, Jarzynski C, Smith SB, Tinoco I Jr, Bustamante C (2005)  
310 Verification of the Crooks fluctuation theorem and recovery of RNA folding free

- 311 energies. *Nature* 437(7056):231–234.
- 312 31. Lussis P, Svaldo-Lanero T, Bertocco A, Fustin C-A, Leigh DA, Duwez A-S (2011) A  
313 single synthetic small molecule that generates force against a load. *Nat Nanotechnol*  
314 6(9):553–557.
- 315 32. Zhu Z, Bruns CJ, Li H, Lei J, Ke C, Liu Z, Shafaie S, Colquhoun HM, Stoddart JF  
316 (2013) Synthesis and solution-state dynamics of donor–acceptor oligorotaxane  
317 foldamers. *Chem Sci* 4(4):1470.
- 318 33. Bruns CJ, Stoddart JF (2013) Mechanically interlaced and interlocked donor–acceptor  
319 foldamers. *Hierarchical Macromolecular Structures: 60 Years after the Staudinger*  
320 *Nobel Prize I*, pp 271–294.
- 321 34. Basu S, Coskun A, Friedman DC, Olson MA, Benítez D, Tkatchouk E, Barin G, Yang  
322 J, Fahrenbach AC, Goddard WA III, Stoddart JF (2011) Donor-acceptor oligorotaxanes  
323 made to order. *Chem - A Eur J* 17(7):2107–2119.
- 324 35. Zhu Z, Li H, Liu Z, Lei J, Zhang H, Botros YY, Stern CL, Sarjeant AA, Stoddart JF,  
325 Colquhoun M (2012) Oligomeric pseudorotaxanes adopting infinite-chain lattice  
326 superstructures. *Angew Chem Int Ed* 51(29):7231–7235.
- 327 36. Beyer MK, Clausen-Schaumann H (2005) Mechanochemistry: The mechanical  
328 activation of covalent bonds. *Chem Rev* 105(8):2921–2948.
- 329 37. Bruns CJ, Stoddart JF (2016) An introduction to the mechanical bond. *The Nature of*  
330 *the Mechanical Bond* (John Wiley & Sons, Inc., Hoboken, NJ, USA), pp 1–54.
- 331 38. Bruns CJ, Stoddart JF (2016) The fundamentals of making mechanical bonds. *The*  
332 *Nature of the Mechanical Bond* (John Wiley & Sons, Inc., Hoboken, NJ, USA), pp 55–  
333 268.
- 334 39. Choi JW, Flood AH, Steuerman DW, Nygaard S, Braunschweig AB, Moonen NN,  
335 Laursen BW, Luo Y, Delonno E, Peters AJ, Jeppesen JO, Xu K, Stoddart JF, Heath JR

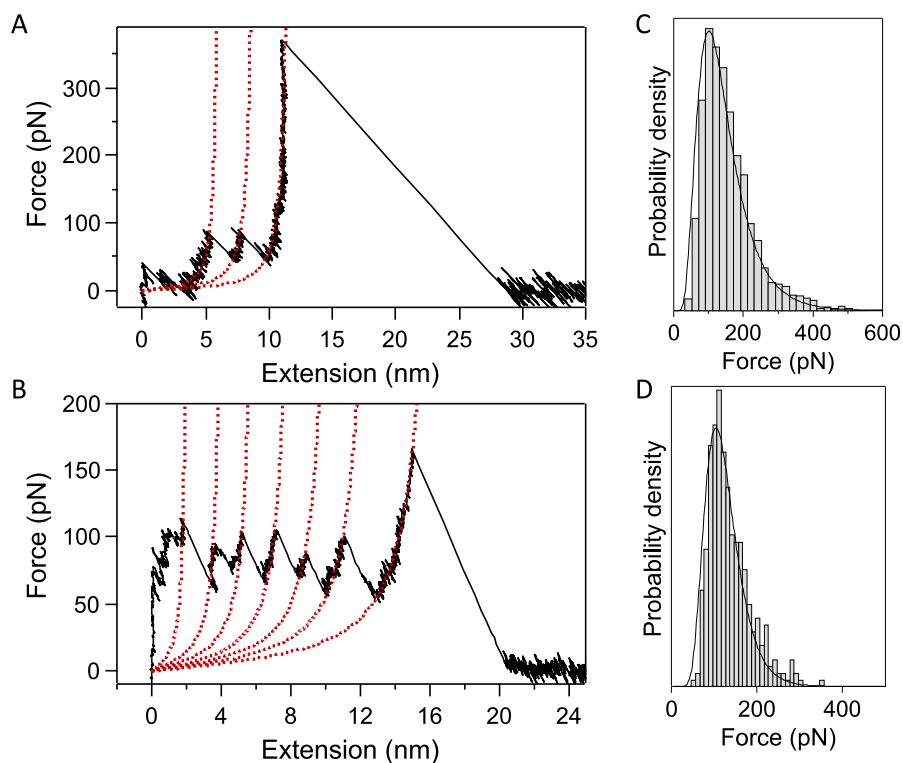
- 336 (2006) Ground-state equilibrium thermodynamics and switching kinetics of bistable  
337 [2]rotaxanes switched in solution, polymer gels, and molecular electronic devices.  
338 *Chem Eur J* 12(1):261-279.
- 339 40. Hugel T, Holland NB, Cattani A, Moroder L, Seitz M, Gaub HE (2002) Single-  
340 molecule optomechanical cycle. *Science* 296(5570):1103–1106.
- 341 41. Shi W, Giannotti MI, Hempenius MA, Schönherr H, Vancso GJ (2007) Closed  
342 mechanochemical cycles of individual single-chain macromolecular motors by  
343 AFM. *Angew Chemie Int Ed* 46(44):8400–8404.
- 344 42. Janke M, Rudzevich Y, Molokanova O, Metzroth T, Mey I, Diezemann G, Marszalek  
345 PE, Gauss J, Böhmer V, Janshoff A (2009) Mechanically interlocked calix[4]arene  
346 dimers display reversible bond breakage under force. *Nat Nanotechnol* 4(4):225–229.
- 347 43. Van Quaethem A, Lussis P, Leigh DA, Duwez A-S, Fustin C-A (2014) Probing the  
348 mobility of catenane rings in single molecules. *Chem Sci* 5(4):1449–1452.
- 349 44. Chung J, Kushner AM, Weisman AC, Guan Z (2014) Direct correlation of single-  
350 molecule properties with bulk mechanical performance for the biomimetic design of  
351 polymers. *Nat Mater* 13(11):1055–1062.
- 352 45. te Riet J, Katan AJ, Rankl C, Stahl SW, van Buul AM, Phang IY, Gomez-Casado A,  
353 Schon P, Gerritsen JW, Cambi A, Rowan AE, Vancso GJ, Jonkheijm P, Huskens J,  
354 Oosterkamp TH, Gaub H, Hinterdorfer P, Figdor CG, Speller S (2011) Interlaboratory  
355 round robin on cantilever calibration for AFM force spectroscopy. *Ultramicroscopy*  
356 111:1659–1669.
- 357 46. Sader JE, Sanelli JA, Adamson BD, Monty JP, Wei X, Crawford SA, Friend JR,  
358 Marusic I, Mulvaney P, Bieske EJ (2012) Spring constant calibration of atomic force  
359 microscope cantilevers of arbitrary shape. *Rev Sci Instrum* 83(10):103705.
- 360

361 **FIGURES AND LEGENDS**



362

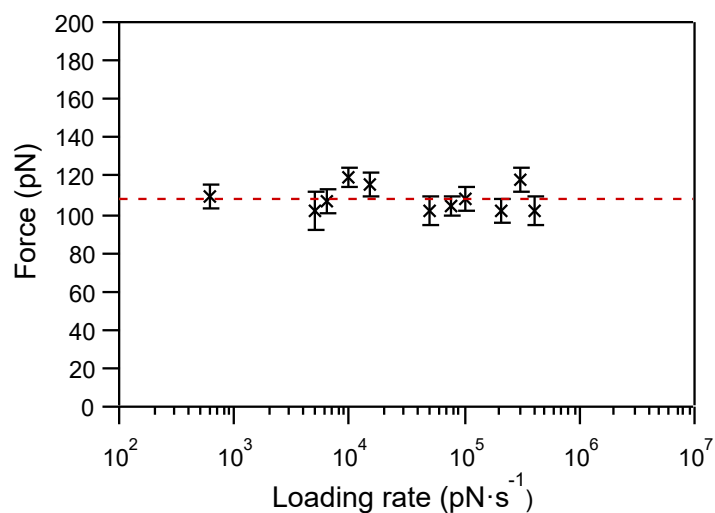
363 **Fig. 1.** Structural formulas of the oligorotaxanes and schematic description of the AFM-based  
 364 single-molecule force spectroscopy experiment. (A,B) Structure formulas and co-  
 365 conformations of the [4]rotaxane (A) and [7]rotaxane (B) of the  $[0.5(n-1)+2]$  family. The  
 366 terms in square brackets denote the total number of interlocked components and  $n$  is the  
 367 number of DNP units present in the backbone components. In this co-conformation, half of  
 368 the dioxynaphthalene (DNP) units (in red) are encircled by cyclobis(paraquat-*p*-phenylene)  
 369 (CBPQT<sup>4+</sup>) rings (in blue). Noncovalent intramolecular interactions such as  $\pi$ -interactions  
 370 linking dioxynaphthalene (DNP) units (in red) and tetracationic cyclobis(paraquat-*p*-  
 371 phenylene) (Blue Boxes), hydrogen bonds linking  $\alpha$ -hydrogen atoms of the Blue Boxes with  
 372 tetra(ethylene oxide) chains in the backbone, and Coulombic interactions between the  
 373 molecular rings and PF<sub>6</sub><sup>-</sup> counterions stabilize the folded conformation. PF<sub>6</sub><sup>-</sup> counterions are  
 374 not shown. (C) Mechanical unfolding of individual oligorotaxanes, leading to the breaking of  
 375 the intramolecular interactions maintaining the folded conformation.



376

377 **Fig. 2.** Characteristic force-extension curves of a [4]- (A) and [7]rotaxane (B) mechanically  
378 stretched at  $7.5 \times 10^4 \text{ pN}\cdot\text{s}^{-1}$  in DMF, showing equally spaced force peaks, each separated by  
379 2.4 nm. Distribution of rupture force for the pulling of the [4]- (C) and [7]rotaxane (B) in  
380 DMF at  $7.5 \times 10^4 \text{ pN}\cdot\text{s}^{-1}$ . The most probable values were obtained by lognormal fits and peak  
381 at  $101.2 \pm 1.2 \text{ pN}$  ( $N = 3338$ ) (C) and  $104 \pm 4.5 \text{ pN}$  ( $N = 362$ ) (D).

382



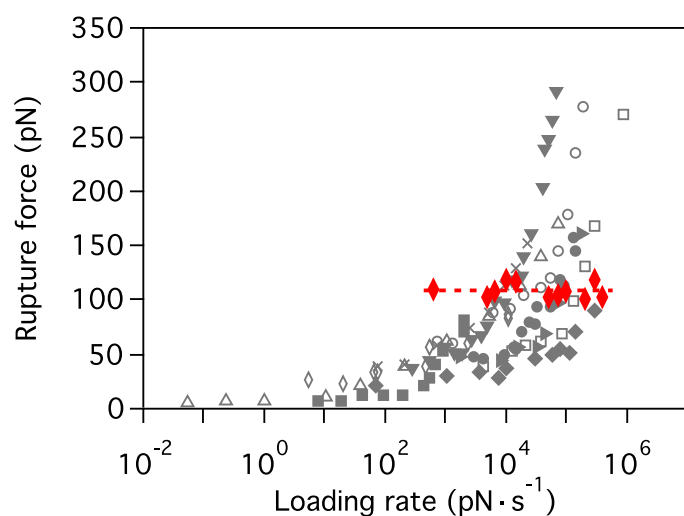
383

384

385 **Fig. 3.** Dynamic force spectrum of the mechanical unfolding of the [4]rotaxane in DMF at 11  
386 loading rates (from  $6 \times 10^2 \text{ pN}\cdot\text{s}^{-1}$  to  $4 \times 10^5 \text{ pN}\cdot\text{s}^{-1}$ ). Each data ( $N \geq 150$ ) is associated with its  
387 effective loading rate and its most probable rupture force (see Fig. S1). As shown by the  
388 horizontal red line ( $F_{eq} = 108.1 \pm 1.2 \text{ pN}$ ), the rupture force does not increase with the loading  
389 rate, establishing the near-equilibrium regime of the experiment.

390

391



392

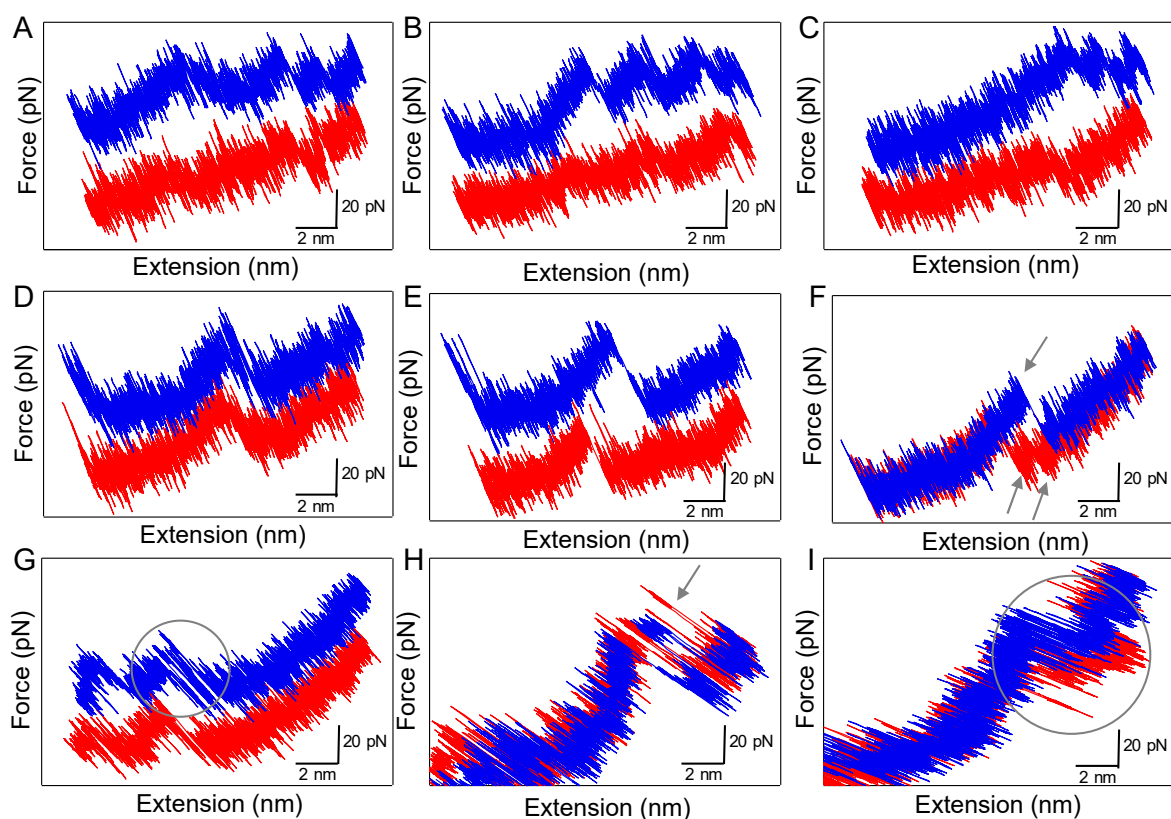
393 **Fig. 4.** Force spectrum of the mechanical unfolding of the [4]rotaxane in DMF (in red)  
394 superimposed with force spectra of 10 data sets (in grey scale) taken from the literature and fit  
395 to the Friddle-Noy-De Yoreo model (adapted from ref. 23). The kinetic regime is not reached  
396 yet at the highest loading rates and the equilibrium force ( $F_{eq} = 108.1\text{pN}$ ) is high compared to  
397 previous studies on natural biomolecules.

398

399

400

401



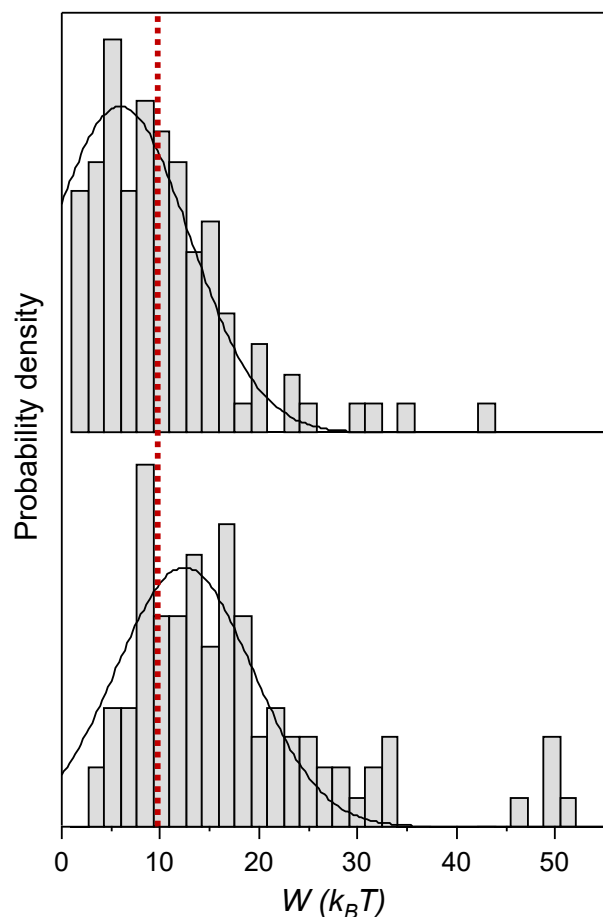
402

403 **Fig. 5.** Stochastic behavior of a single [7]rotaxane during pulling (blue)-relaxing (red)  
 404 experiments in DMF (the pulling traces A-E and G are shown with a 30 pN-offset for more  
 405 clarity). These curves exhibit the recovery of the characteristic sawtooth pattern during the  
 406 relaxation step (A-C), the reversible breaking of a single interaction without (D) and with (E)  
 407 hysteresis, the simultaneous breaking of two interactions and their subsequent reforming (F),  
 408 and the presence of fluctuations between folded and unfolded states during the pulling and the  
 409 relaxing curves (G-I).

410

411

412



413

414 **Fig. 6.** Distributions of forward (pulling step, lower panel) and reverse (relaxing step, upper  
415 panel) works corresponding, respectively, to the breaking and the reforming of a single  
416 interaction within the folded [4]rotaxane in DMF ( $N = 96$ ). These distributions were obtained  
417 from pulling-relaxing experiments in the near-equilibrium regime (loading rate of  $10^3$  pN·s<sup>-1</sup>).  
418 Gaussian fits of the raw data are superimposed with the histograms (bin size =  $0.5 k_B T$ ). The  
419 distributions have the same value (red line) at  $W = 10 \pm 2 k_B T$  or  $6 \pm 1$  kcal·mol<sup>-1</sup>.

420